axioms

MDPI

Article

A Novel Computational Framework for Time-Fractional Higher-Order KdV Models: CLADM-Based Solutions and Comparative Analysis

Priti V. Tandel [1], Anant Patel [1,†] and Trushitkumar Patel [2,*,†]

[1] Department of Mathematics, Veer Narmad South Gujarat University, Surat 395007, Gujarat, India; pvtandel@vnsgu.ac.in (P.V.T.); aspatel@vnsgu.ac.in (A.P.)
[2] Department of General Studies, University of the People, Pasadena, CA 91101, USA
* Correspondence: trushitkumar.patel@uopeople.edu
† These authors contributed equally to this work.

Abstract

This study applies the Conformable Laplace Adomian Decomposition Method (CLADM) to solve generalized time-fractional Korteweg–de Vries (KdV) models, including seventh- and fifth-order models. CLADM combines the conformable fractional derivative and Laplace transform with the Adomian decomposition technique, offering analytic approximate solutions. Numerical and graphical results, generated using MATLAB R2020a 9.8.0.1323502, validate the method's efficiency and precision in capturing fractional-order dynamics. Fractional parameters ϱ significantly influence wave behavior, with higher orders yielding smoother profiles and reduced oscillations. Comparative analysis confirms CLADM's superiority over existing methods in minimizing errors. The versatility of CLADM highlights its potential for studying nonlinear wave phenomena in diverse applications.

Keywords: nonlinear wave dynamics; time-fractional higher order KdV equations; conformable laplace adomian decomposition method

MSC: 35R11; 35Q53

check for updates

Academic Editor: Patricia J. Y. Wong

Received: 22 May 2025
Revised: 20 June 2025
Accepted: 25 June 2025
Published: 1 July 2025

Citation: Tandel, P.V.; Patel, A.; Patel, T. A Novel Computational Framework for Time-Fractional Higher-Order KdV Models: CLADM-Based Solutions and Comparative Analysis. *Axioms* **2025**, *14*, 511. https://doi.org/10.3390/axioms14070511

Copyright: © 2025 by the authors. Licensee MDPI, Basel, Switzerland. This article is an open access article distributed under the terms and conditions of the Creative Commons Attribution (CC BY) license (https://creativecommons.org/licenses/by/4.0/).

1. Introduction

The Korteweg–de Vries (KdV) model is a fundamental nonlinear partial differential equation that arises in the study of shallow water waves, plasma physics, and other physical systems. The KdV model is vital in understanding nonlinear wave dynamics across diverse physical phenomena, including flood analysis, plasma waves, and ocean surface waves. In ocean engineering, they are crucial for predicting tsunami wave evolution, understanding internal waves in stratified fluids, and analyzing rogue waves, all of which are essential for ensuring the stability of offshore structures and coastal protection. Furthermore, these models are particularly valuable for studying coastal wave dynamics and interactions between offshore structures and waves, offering critical insights for designing resilient coastal and marine infrastructure. Beyond fluid dynamics, the KdV model has significantly influenced several scientific domains, such as optics, quantum field theory, general relativity, plasma physics, and fluid mechanics. The origins of solitary wave research trace back to Russell's discovery in 1834, during their observations of water waves while working on canal boat designs. Subsequent investigations by Boussinesq and Rayleigh in the 1870s provided critical insights that eventually led to the formulation of the classical KdV model by Korteweg

and de Vries in 1895. Since then, various extensions and adaptations of the KdV model have emerged, including the modified KdV (mKdV), fifth-order KdV, generalized KdV and Hirota–Satsuma KdV equations. These variations have been introduced to address complex physical scenarios and enhance the applicability of the original model [1].

The seventh-order KdV model extends the classical KdV framework by incorporating higher-order dispersion and nonlinearity terms, enabling the modeling of more intricate wave phenomena. Researchers have applied the Adomian Decomposition Method (ADM) to approximate solutions of seventh-order KdV equations, enhancing the analytical tools available for complex nonlinear differential Equations [2]. The Homotopy Analysis Method (HAM) has also been utilized to derive approximate solutions, demonstrating the equation's role in advancing analytical techniques for higher-order nonlinear problems [3]. The seventh-order KdV model has been analyzed to identify conservation laws, which are crucial for understanding the invariants and symmetries of complex nonlinear systems [4]. Studies have explored generalized solitary wave solutions within the framework of higher-order KdV models, including the seventh-order variant. These investigations contribute to the broader understanding of solitary wave behavior in nonlinear systems [5]. Ozkan derived exact solutions for the time-fractional seventh-order Sawada–Kotera–Ito model using the exp-function, (G'/G)-expansion, and ansatz methods, yielding dark, bright, and singular soliton solutions [6]. Mancas and Hereman investigated traveling-wave solutions to fifth- and seventh-order KdV models using elliptic function methods. Their research offers exact solutions that serve as benchmarks for numerical solvers and aid in understanding the dynamics of nonlinear wave models [7]. Research has been conducted on a seventh-order generalized KdV model and its fractional version in fluid mechanics using symmetry analysis. This work aids in understanding the role of symmetries in the solutions and conservation laws of higher-order KdV models [8].

The LADM has been employed to obtain numerical and approximate solutions for certain fifth-order KdV equations. This method integrates Laplace transforms with Adomian polynomials to efficiently manage nonlinear terms [9]. Studies have explored new closed-form solutions of the time-fractional fifth-order KdV model using Lie group analysis and the G'/G-expansion method, providing insights into the behavior of fractional-order nonlinear systems [10]. The trial equation method has been utilized to the fifth-order KdV equation to find exact solutions, aiding in the analysis of complex dynamic behaviors in fractional calculus [11]. The extended complex method has been utilized to explore exact solutions for the generalized fifth-order KdV model, providing insights into the equation's integrability and solution structures [12]. The authors investigated the nonlinear variable-order fractional KdV equation, which models shallow water waves. They employed the modified (G'/G)-expansion method to derive exact solitary wave solutions and traveling wave solutions. The study contributes to the understanding of wave dynamics in shallow water by providing analytical solutions to this fractional differential Equation [13]. The authors investigated the generalized fifth-order KdV model, with fifth-order linear dispersion and cubic nonlinearity terms. They employed the modified exp-function method to derive exact traveling wave solutions, including solitary wave solutions. The study contributes to the understanding of wave dynamics in shallow water by providing analytical solutions to this nonlinear partial differential Equation [14]. The study explores the Kaup–Kupershmidt (KK) model, a particular variant of the fifth-order KdV model. The authors formulated the equation using a Lagrangian framework, derived associated conservation laws, and determined exact analytical solutions for ocean gravity waves described by this equation. This research provides valuable insights into the dynamics of waves in shallow water by presenting both analytical solutions and conservation principles for the KK model [15]. The authors proposed a robust fuzzy double parametric approach, specifically the q-Homotopy

Analysis Shehu Transform Method (q-HAShTM), to solve the generalized fuzzy fractional KdV equation. This method incorporates Hukuhara differentiability and Shehu transform to handle uncertainties in the velocity profiles at various spatial positions [16].

Fractional KdV equations have been widely studied due to their significance in modeling nonlinear wave dynamics in various physical systems, including shallow water waves, ion-acoustic waves in plasma, and optical solitons. Researchers have applied various analytical and numerical techniques to study different forms of fractional KdV equations. Kurulay and Bayram employed the Differential Transform Method (DTM) to obtain approximate analytical solutions for the fractional modified KdV (fmKdV) and fractional KdV (fKdV) equations based on the Caputo fractional derivative [17]. Wang applied Lie symmetry analysis to the time-fractional fifth-order KdV equation, transforming it into an ordinary differential equation involving the Erdelyi–Kober fractional derivative [18]. Nazari-Golshan investigated the Space-Fractional Modified KdV (SFMKdV) equation using the Modified G'/G-expansion method, showing how space-fractional parameters influence ion acoustic wave propagation [19]. Alshammari investigated a fractional-order system of KdV equations using the Modified Decomposition Method (MDM) and the New Iterative Transform Method (NITM), demonstrating their effectiveness in obtaining accurate analytical approximations while reducing computational costs [20]. Cao developed efficient finite difference schemes for solving the time-fractional KdV equation, proving their unique solvability, boundedness, and high convergence order [21]. Yousif applied a conformable-Caputo fractional nonpolynomial spline method, enhancing computational efficiency for solving fractional KdV Equations [22]. Dwivedi and Sarkar developed a Crank–Nicolson Fourier-spectral-Galerkin scheme, ensuring the preservation of integral invariants in long-term simulations of fractional KdV-type models [23]. Gu introduced a local discontinuous Galerkin method with generalized alternating numerical fluxes, improving numerical accuracy in fractional KdV models [24].

Moreover, while several studies have used fractional derivatives such as Caputo, Riemann–Liouville, and Erdelyi–Kober, the use of conformable fractional derivatives remains an area of active research due to their computational simplicity and ability to approximate fractional-order behavior effectively. Khalil [25] introduced the conformable fractional derivative (CFD), a modern extension of the traditional limit-based definition of a derivative. Owing to its simplicity, this derivative has been extensively applied in conjunction with various methods [26–29] across numerous contexts. This study employs the Conformable Laplace Adomian Decomposition Method (CLADM) to solve generalized time-fractional KdV models, focusing on seventh- and fifth-order models. Specifically, we examine the fifth-order time-fractional KdV Sawada–Kotera (SK) model, the time-fractional seventh-order KdV Sawada–Kotera–Ito (SKI) model, Kaup–Kuperschmidt (KK) model, and Lax model. These models are highly significant for modeling nonlinear wave phenomena, particularly in oceanography and ocean engineering, where they describe the propagation of shallow water waves, solitons, and other dispersive wave behaviors. The fractional-order derivatives in these equations provide a more accurate representation of complex physical processes, such as wave dispersion and dissipation, which are vital for understanding ocean dynamics and mitigating risks in coastal engineering projects. To validate our approach, we compare the CLADM solutions with exact solutions both numerically and graphically, demonstrating the method's accuracy and efficiency. The CLADM is chosen for its ability to handle nonlinear fractional differential equations effectively, offering advantages such as reduced computational complexity, high precision in approximating solutions, and the ability to provide analytical solutions in series form. This makes CLADM particularly well-suited for solving complex fractional-order models like the ones studied here. Our work

not only advances the theoretical understanding of these models but also provides practical tools for analyzing real-world phenomena in oceanography and ocean engineering.

The remainder of this article is structured as follows. Section 2 discusses the concept of CLADM for fractional PDEs. Section 3 applies CLADM to KdV models. Section 4 presents the numerical results obtained by CLADM. Conclusions are outlined in Section 5.

2. Concept of CLADM for FPDEs

Definition 1 (see [25]). *Given a function $\Omega : [0,\infty) \to \mathbb{R}$, then the Conformable Fractional Derivative of order ϱ is given by*

$$\left(\mathfrak{T}_{\varrho}\Omega\right)(\tau) = \lim_{\epsilon\to 0} \frac{\Omega(\tau + \epsilon\,\tau^{1-\varrho}) - \Omega(\tau)}{\epsilon},$$

for all $\tau > 0,\ \varrho \in (0,1]$.

Definition 2 (see [30]). *Let Ω is an n times differentiable at τ. Then, the conformable fractional derivative of Ω of order ϱ is defined as:*

$$\left(\mathfrak{T}_{\varrho}\,\Omega\right)(\tau) = \lim_{\epsilon\to 0} \frac{\Omega^{([\varrho]-1)}\left(\tau + \epsilon\tau^{([\varrho]-\varrho)}\right) - \Omega^{([\varrho]-1)}(\tau)}{\epsilon},$$

for all $\tau > 0,\ \varrho \in (n, n+1],\ n > 0$ and $[\varrho]$ is the smallest integer greater than or equal to ϱ.

Let us next investigate the basic fractional Laplace transform [30].

Definition 3 (see [30,31]). *Let $\varrho \in (0,1]$ and $\Omega\colon [0,\infty) \to \mathbb{R}$ be real valued function. Then, the Laplace transform for fractional order ϱ is defined by:*

$$\mathfrak{L}_{\varrho}[\Omega(\tau)](s) = \int_0^{\infty} E_{\varrho}(-s,\tau)\Omega(\tau)\, d_{\varrho}\tau, \tag{1}$$

where $E_{\varrho}(-s,\tau) = exp\left(-s\,\frac{\tau^{\varrho}}{\varrho}\right)$.

The Laplace transform in the conformable fractional-order sense is described as

$$\mathfrak{L}_{\varrho}[\mathfrak{D}_{\tau}^{(\varrho)}\Omega(\tau)] = s\mathfrak{L}_{\varrho}[\Omega(\tau)] - \Omega(0), \tag{2}$$

The usual and fractional Laplace transform has the following relation.

Theorem 1 (see [31]). *Let $\Omega\colon [0,\infty) \to \mathbb{R}$ be a function, and if $\mathfrak{L}_{\varrho}\Omega(\tau)(s) = \Theta\varrho(s)$ exists, then*

$$\Theta_{\varrho}(s) = \mathcal{L}\left[\Omega\left((\varrho\tau)^{1/\varrho}\right)\right](s), \tag{3}$$

where $\mathcal{L}[G(\tau)](s) = \int_0^{\infty} e^{-s\tau}G(\tau)\, d\tau$.

Theorem 2 (see [32,33]). *If $\Omega(\xi,\tau) = \sum_{k=0}^{\infty}\Phi_k(\xi)\tau^k$ is a given series;*

1. *If $\exists\ 0 < \sigma < 1$ such that $\frac{\|\Phi_{k+1}\|}{\|\Phi_k\|} \le \sigma$, then the given series solution is convergent.*
2. *If $\exists\ \sigma > 1$ such that $\frac{\|\Phi_{k+1}\|}{\|\Phi_k\|} \ge \sigma$, then the given series solution is divergent.*

Consider the following FPDEs forms:

$$\mathfrak{D}_{\tau}^{\varrho}\Omega(\xi,\tau) + \mathfrak{D}_{\xi}^{\eta}\Omega(\xi,\tau) + \mathcal{R}(\Omega(\xi,\tau)) + \mathcal{N}(\Omega(\xi,\tau)) = g(\xi,\tau), \tag{4}$$

where $\xi > 0,\ \tau > 0,\ 0 < \varrho \leq 1$.

The fractional derivative $\mathfrak{D}_{\tau}^{\varrho}$ in Equation (4) is considered in the conformable sense in τ, $\mathfrak{D}_{\xi}^{n}$ is the highest-order classical derivative operator in ξ, $\mathcal{R}$ is other lower-order derivative terms, $\mathcal{N}$ is the nonlinear term, and $g(\xi,\tau)$ is the sources term with the initial condition.

$$\Omega(\xi,0) = f(\xi), \tag{5}$$

Applying the conformable Laplace transform $\mathfrak{L}_{\varrho}$ with respect to τ both sides of Equation (4), we have

$$\mathfrak{L}_{\varrho}[\mathfrak{D}_{\tau}^{\varrho}\Omega] + \mathfrak{L}_{\varrho}[\mathfrak{D}_{\xi}^{n}\Omega] + \mathfrak{L}_{\varrho}[\mathcal{R}(\Omega) + \mathcal{N}(\Omega)] = \mathfrak{L}_{\varrho}[g(\xi,\tau)], \tag{6}$$

By applying property Equation (2) of conformable Laplace transform, Equation (6) becomes

$$s\mathfrak{L}_{\varrho}[\Omega] - \Omega(\xi,0) + \mathfrak{L}_{\varrho}[\mathfrak{D}_{\xi}^{n}\Omega] + \mathfrak{L}_{\varrho}[\mathcal{R}(\Omega) + \mathcal{N}(\Omega)] = \mathfrak{L}_{\varrho}[g(\xi,\tau)], \tag{7}$$

Which can be written as,

$$\mathfrak{L}_{\varrho}[\Omega] = \frac{1}{s}\left[\Omega(\xi,0) + \mathfrak{L}_{\varrho}\{g(\xi,\tau)\}\right] - \frac{1}{s}\mathfrak{L}_{\varrho}[\mathfrak{D}_{\xi}^{n}\Omega] - \frac{1}{s}\mathfrak{L}_{\varrho}[\mathcal{R}(\Omega) + \mathcal{N}(\Omega)], \tag{8}$$

In Equation (8), applying inverse Laplace transform in conformable sense, we have

$$\begin{aligned} \Omega(\xi,\tau) \quad = \quad & \mathfrak{L}_{\varrho}^{-1}\left[\tfrac{1}{s}\left[\Omega(\xi,0) + \mathfrak{L}_{\varrho}\{g(\xi,\tau)\}\right]\right] - \mathfrak{L}_{\varrho}^{-1}\left[\tfrac{1}{s}\mathfrak{L}_{\varrho}\left\{\mathfrak{D}_{\xi}^{n}\Omega\right\}\right] \\ & -\mathfrak{L}_{\varrho}^{-1}\left[\tfrac{1}{s}\mathfrak{L}_{\varrho}\{\mathcal{R}(\Omega) + \mathcal{N}(\Omega)\}\right], \end{aligned} \tag{9}$$

where the nonlinear term $\mathcal{N}(\Omega)$ of Equation (4) is handled by applying ADM and the solution is expressed as an infinite sum of series:

$$\Omega(\xi,\tau) = \sum_{k=0}^{\infty}\Omega_k(\xi,\tau), \tag{10}$$

$$\mathcal{N}(\Omega(\xi,\tau)) = \sum_{k=0}^{\infty}A_k, \tag{11}$$

where Adomian polynomials A_k are given by,

$$A_k = \frac{1}{k!}\frac{d^k}{d\lambda^k}\left[\mathcal{N}\left(\sum_{j=0}^{k}\lambda^j\Omega_j\right)\right]\Bigg|_{\lambda=0}, \quad k = 0,1,2,3,\ldots \tag{12}$$

By substituting Equations (10) and (11) into Equation (9),

$$\begin{aligned} \textstyle\sum_{k=0}^{\infty}\Omega_k \quad = \quad & \mathfrak{L}_{\varrho}^{-1}\left[\tfrac{1}{s}\left[\Omega(\xi,0) + \mathfrak{L}_{\varrho}\{g(\xi,\tau)\}\right]\right] - \mathfrak{L}_{\varrho}^{-1}\left[\tfrac{1}{s}\mathfrak{L}_{\varrho}\left\{\textstyle\sum_{k=0}^{\infty}\mathfrak{D}_{\xi}^{n}\Omega_k\right\}\right] \\ & -\mathfrak{L}_{\varrho}^{-1}\left[\tfrac{1}{s}\mathfrak{L}_{\varrho}\{\mathcal{R}(\textstyle\sum_{k=0}^{\infty}\Omega_k) + \textstyle\sum_{k=0}^{\infty}A_k\}\right], \end{aligned} \tag{13}$$

When comparing both sides of Equation (13), we get the following recursive relation:

$$\Omega_0 = \mathfrak{L}_{\varrho}^{-1}\left[\frac{1}{s}\left[\Omega(\xi,0) + \mathfrak{L}_{\varrho}\{g(\xi,\tau)\}\right]\right], \tag{14}$$

$$\Omega_1 = -\mathfrak{L}_{\varrho}^{-1}\left[\frac{1}{s}\mathfrak{L}_{\varrho}\left\{\mathfrak{D}_{\xi}^{n}\Omega_0\right\}\right] - \mathfrak{L}_{\varrho}^{-1}\left[\frac{1}{s}\mathfrak{L}_{\varrho}\{\mathcal{R}(\Omega_0) + A_0\}\right], \tag{15}$$

$$\Omega_2 = -\mathfrak{L}_{\varrho}^{-1}\left[\frac{1}{s}\mathfrak{L}_{\varrho}\left\{\mathfrak{D}_{\xi}^{n}\Omega_1\right\}\right] - \mathfrak{L}_{\varrho}^{-1}\left[\frac{1}{s}\mathfrak{L}_{\varrho}\{\mathcal{R}(\Omega_1) + A_1\}\right], \tag{16}$$

In general, the relation can be written as

$$\Omega_{k+1} = -\mathfrak{L}_{\varrho}^{-1}\left[\frac{1}{s}\mathfrak{L}_{\varrho}\left\{\mathfrak{D}_{\xi}^{\eta}\,\Omega_k\right\}\right] - \mathfrak{L}_{\varrho}^{-1}\left[\frac{1}{s}\mathfrak{L}_{\varrho}\{\mathcal{R}(\Omega_k) + A_k\}\right]. \tag{17}$$

where $k = 0, 1, 2, 3, \ldots$

The solution $\Omega(\xi, \tau)$ can be obtained from Equation (10).

3. Application of CLADM on KdV Time-Fractional Models

This study extends the CLADM to solve fifth-order time-fractional KdV models, specifically the SK model. This model can be expressed in the form of the generalized fifth-order time-fractional KdV equation:

$$\mathfrak{D}_{\tau}^{\varrho}\Omega + \eta_1\,\Omega^2\,\Omega_{\xi} + \eta_2\,\Omega_{\xi}\,\Omega_{\xi\xi} + \eta_3\,\Omega\,\Omega_{\xi\xi\xi} + \Omega_{\xi\xi\xi\xi\xi} = 0, \tag{18}$$

where $\varrho \in (0, 1]$ and η_i's are arbitrary and nonzero parameters. The well-known Sawada–Kotera model is obtained by setting $\eta_1 = 45$, $\eta_2 = 15$, $\eta_3 = 15$ and $\eta_4 = 1$ in Equation (18) [34,35].

A general form of time-fractional seventh-order KdV model is written by [1]:

$$\begin{aligned}\mathfrak{D}_{\tau}^{\varrho}\Omega + \eta_1\,\Omega^3\,\Omega_{\xi} + \eta_2\,\Omega_{\xi}{}^3 + \eta_3\,\Omega\,\Omega_{\xi}\,\Omega_{\xi\xi} + \eta_4\,\Omega^2\,\Omega_{\xi\xi\xi} + \eta_5\,\Omega_{\xi\xi}\,\Omega_{\xi\xi\xi} + \\ \eta_6\,\Omega_{\xi}\,\Omega_{\xi\xi\xi\xi} + \eta_7\,\Omega\,\Omega_{\xi\xi\xi\xi\xi} + \Omega_{\xi\xi\xi\xi\xi\xi\xi} = 0,\end{aligned} \tag{19}$$

where $\varrho \in (0, 1]$ and η_is are arbitrary and nonzero parameters.

Example 1. *Consider the time fractional fifth-order KdV SK model:*

$$\mathfrak{D}_{\tau}^{\varrho}\Omega + 45\,\Omega^2\,\Omega_{\xi} + 15\,\Omega_{\xi}\,\Omega_{\xi\xi} + 15\,\Omega\,\Omega_{\xi\xi\xi} + \Omega_{\xi\xi\xi\xi\xi} = 0, \tag{20}$$

where $\varrho \in (0, 1]$ *and subject to the initial condition*

$$\Omega(\xi, 0) = 2\,\delta^2\,\operatorname{sec}h^2(\delta\xi). \tag{21}$$

Solution: By applying CLADM on Equation (20) discussed in Section 2, we can have

$$\begin{aligned}\Omega(\xi,\tau) \;=\; & -\mathfrak{L}_{\varrho}^{-1}\left[\tfrac{1}{s}\mathfrak{L}_{\varrho}\left(\Omega(\xi,0) + \Omega_{\xi\xi\xi\xi\xi}\right)\right] - \mathfrak{L}_{\varrho}^{-1}\left[\tfrac{1}{s}\mathfrak{L}_{\varrho}\left(45\,\Omega^2\,\Omega_{\xi}\right.\right. \\ & \left.\left. +15\,\Omega_{\xi}\,\Omega_{\xi\xi} + 15\,\Omega\,\Omega_{\xi\xi\xi}\right)\right],\end{aligned} \tag{22}$$

$$\begin{aligned}\Omega_{k+1} \;=\; & -\mathfrak{L}_{\varrho}^{-1}\left[\tfrac{1}{s}\mathfrak{L}_{\varrho}\left(\Omega(\xi,0) + \Omega_{\xi\xi\xi\xi\xi_k}\right)\right] - \mathfrak{L}_{\varrho}^{-1}\left[\tfrac{1}{s}\mathfrak{L}_{\varrho}(45\,\textstyle\sum_{k=0}^{\infty} A_k\right. \\ & \left. +15\,\textstyle\sum_{k=0}^{\infty} B_k + 15\,\sum_{k=0}^{\infty} C_k)\right],\end{aligned} \tag{23}$$

From the initial condition Equation (21), we get

$$\Omega_0(\xi, \tau) = \Phi_0(\xi) = 2\,\delta^2\,\operatorname{sec}h^2(\delta\xi), \tag{24}$$

$$\Omega_1(\xi, \tau) = \Phi_1(\xi)\tau^{\varrho} = \frac{64\,\delta^7 \operatorname{sech}(\delta\xi)^2 \tanh(\delta\xi)\tau^{\varrho}}{\varrho}, \tag{25}$$

$$\Omega_2(\xi, \tau) = \Phi_2(\xi)\tau^{2\varrho} = -\frac{512\,\tau^{2\varrho}\delta^{12}\operatorname{sech}(\delta\xi)^2\left(3\operatorname{sech}(\delta\xi)^2 - 2\right)}{\varrho^2}, \tag{26}$$

$$\Omega_3(\xi,\tau)=\Phi_3(\xi)\tau^{3\varrho}=\frac{32768\,\delta^{17}\mathrm{sech}(\delta\xi)^4\tanh(\delta\xi)\tau^{3\varrho}\left(\cosh^2(\delta\xi)-3\right)}{3\varrho^3}, \tag{27}$$

The solution of Equation (20) is obtained in the form of Equation (10).

The exact solution of Equation (20) is given by:

$$\Omega(\xi,\tau)=2\,\delta^2\,\mathrm{sec}\,h^2\left(\delta\xi-16\delta^4\tau\right),$$

Example 2. *Consider the time fractional seventh-order KdV KK model (by setting* $\eta_1=2016$, $\eta_2=630$, $\eta_3=2268$, $\eta_4=504$, $\eta_5=252$, $\eta_6=147$, $\eta_7=42$ *in Equation (19)):*

$$\begin{aligned}&\mathfrak{D}_\tau^\varrho\Omega+2016\,\Omega^3\,\Omega_\xi+630\,\Omega_\xi{}^3+2268\,\Omega\,\Omega_\xi\,\Omega_{\xi\xi}+504\,\Omega^2\,\Omega_{\xi\xi\xi}\\&+252\,\Omega_{\xi\xi}\,\Omega_{\xi\xi\xi}+147\,\Omega_\xi\,\Omega_{\xi\xi\xi\xi}+42\,\Omega\,\Omega_{\xi\xi\xi\xi\xi}+\Omega_{\xi\xi\xi\xi\xi\xi\xi}=0,\end{aligned} \tag{28}$$

where $\varrho\in(0,1]$ *and with initial condition*

$$\Omega(\xi,0)=\frac{\delta^2}{3}-\frac{\delta^2}{2}\tanh^2(\delta\xi). \tag{29}$$

Solution: By applying CLADM on Equation (28) discussed in Section 2, we will have

$$\begin{aligned}\Omega(\xi,\tau) &= -\mathfrak{L}_\varrho^{-1}\left[\tfrac{1}{s}\mathfrak{L}_\varrho\left(\Omega(\xi,0)+\Omega_{\xi\xi\xi\xi\xi\xi\xi}\right)\right]-\mathfrak{L}_\varrho^{-1}\left[\tfrac{1}{s}\mathfrak{L}_\varrho\left(2016\,\Omega^3\,\Omega_\xi\right.\right.\\&\quad+630\,\Omega_\xi{}^3+2268\,\Omega\,\Omega_\xi\,\Omega_{\xi\xi}+504\,\Omega^2\,\Omega_{\xi\xi\xi}+252\,\Omega_{\xi\xi}\,\Omega_{\xi\xi\xi}\\&\quad\left.\left.+147\,\Omega_\xi\,\Omega_{\xi\xi\xi\xi}+42\,\Omega\,\Omega_{\xi\xi\xi\xi\xi}\right)\right],\end{aligned} \tag{30}$$

$$\begin{aligned}\Omega_{k+1} &= -\mathfrak{L}_\varrho^{-1}\left[\tfrac{1}{s}\mathfrak{L}_\varrho\left(\Omega(\xi,0)+\Omega_{\xi\xi\xi\xi\xi\xi\xi_k}\right)\right]-\mathfrak{L}_\varrho^{-1}\left[\tfrac{1}{s}\mathfrak{L}_\varrho(2016\,\textstyle\sum_{k=0}^{\infty}A_k\right.\\&\quad+630\,\textstyle\sum_{k=0}^{\infty}B_k+2268\,\sum_{k=0}^{\infty}C_k+504\,\sum_{k=0}^{\infty}D_k\\&\quad\left.+252\,\textstyle\sum_{k=0}^{\infty}E_k+147\,\sum_{k=0}^{\infty}F_k+42\,\sum_{k=0}^{\infty}G_k)\right],\end{aligned} \tag{31}$$

From the initial condition Equation (29), we get

$$\Omega_0(\xi,\tau)=\Phi_0(\xi)=\frac{\delta^2}{3}-\frac{\delta^2\,\tanh^2(\delta\xi)}{2}, \tag{32}$$

$$\Omega_1(\xi,\tau)=\Phi_1(\xi)\tau^{\varrho}=-\frac{4\,\delta^9\tanh(\delta\xi)\mathrm{sech}(\delta\xi)^2\,\tau^{\varrho}}{3\varrho}, \tag{33}$$

$$\Omega_2(\xi,\tau)=\Phi_2(\xi)\tau^{2\varrho}=-\frac{8\,\delta^{16}\mathrm{sech}(\delta\xi)^2\left(3\mathrm{sech}(\delta\xi)^2-2\right)\tau^{2\varrho}}{9\varrho^2}, \tag{34}$$

$$\Omega_3(\xi,\tau)=\Phi_3(\xi)\tau^{3\varrho}=-\frac{128\,\delta^{23}\left(\cosh^2(\delta\xi)-3\right)\tanh(\delta\xi)\mathrm{sech}(\delta\xi)^4\,\tau^{3\varrho}}{81\varrho^3}, \tag{35}$$

The solution of Equation (28) is obtained in the form of Equation (10).

The exact solution of Equation (28) is given by:

$$\Omega(\xi,\tau)=\frac{\delta^2}{3}-\frac{\delta^2}{2}\tanh^2\left(\delta\xi+\frac{4}{3}\delta^7\tau\right).$$

Example 3. *Consider the time fractional seventh-order KdV SKI model (by setting* $\eta_1 = 252$, $\eta_2 = 63$, $\eta_3 = 378$, $\eta_4 = 126$, $\eta_5 = 63$, $\eta_6 = 42$, $\eta_7 = 21$ *in Equation (19)):*

$$\mathfrak{D}_\tau^\varrho \Omega + 252\,\Omega^3\,\Omega_\xi + 63\,{\Omega_\xi}^3 + 378\,\Omega\,\Omega_\xi\,\Omega_{\xi\xi} + 126\,\Omega^2\,\Omega_{\xi\xi\xi} + 63\,\Omega_{\xi\xi}\,\Omega_{\xi\xi\xi} + 42\,\Omega_\xi\,\Omega_{\xi\xi\xi\xi} + 21\,\Omega\,\Omega_{\xi\xi\xi\xi\xi} + \Omega_{\xi\xi\xi\xi\xi\xi\xi} = 0, \tag{36}$$

where $\varrho \in (0, 1]$ *and with the initial condition*

$$\Omega(\xi, 0) = \frac{4\delta^2}{3}(2 - 3\,\tanh^2(\delta\xi)). \tag{37}$$

Solution: By applying CLADM on Equation (36) discussed in Section 2, we will have

$$\begin{aligned}\Omega(\xi,\tau) \;=\; & -\mathfrak{L}_\varrho^{-1}\Big[\tfrac{1}{s}\mathfrak{L}_\varrho\big(\Omega(\xi,0) + \Omega_{\xi\xi\xi\xi\xi\xi\xi}\big)\Big] - \mathfrak{L}_\varrho^{-1}\Big[\tfrac{1}{s}\mathfrak{L}_\varrho\big(252\,\Omega^3\,\Omega_\xi \\ & +63\,{\Omega_\xi}^3 + 378\,\Omega\,\Omega_\xi\,\Omega_{\xi\xi} + 126\,\Omega^2\,\Omega_{\xi\xi\xi} + 63\,\Omega_{\xi\xi}\,\Omega_{\xi\xi\xi} \\ & +42\,\Omega_\xi\,\Omega_{\xi\xi\xi\xi} + 21\,\Omega\,\Omega_{\xi\xi\xi\xi\xi}\big)\Big],\end{aligned} \tag{38}$$

$$\begin{aligned}\Omega_{k+1} \;=\; & -\mathfrak{L}_\varrho^{-1}\Big[\tfrac{1}{s}\mathfrak{L}_\varrho\big(\Omega(\xi,0) + \Omega_{\xi\xi\xi\xi\xi\xi\xi_k}\big)\Big] - \mathfrak{L}_\varrho^{-1}\Big[\tfrac{1}{s}\mathfrak{L}_\varrho(252\,\textstyle\sum_{k=0}^{\infty} A_k \\ & +63\,\textstyle\sum_{k=0}^{\infty} B_k + 378\,\sum_{k=0}^{\infty} C_k + 126\,\sum_{k=0}^{\infty} D_k \\ & +63\,\textstyle\sum_{k=0}^{\infty} E_k + 42\,\sum_{k=0}^{\infty} F_k + 21\,\sum_{k=0}^{\infty} G_k)\Big],\end{aligned} \tag{39}$$

From the initial condition Equation (37), we get

$$\Omega_0(\xi,\tau) = \Phi_0(\xi) = \frac{4\,\delta^2\Big(2 - 3\,\tanh^2(\delta\xi)\Big)}{3}, \tag{40}$$

$$\Omega_1(\xi,\tau) = \Phi_1(\xi)\tau^\varrho = -\frac{2048\,\delta^9\,\tanh(\delta\xi)\mathrm{sech}(\delta\xi)^2\,\tau^\varrho}{3\varrho}, \tag{41}$$

$$\Omega_2(\xi,\tau) = \Phi_2(\xi)\tau^{2\varrho} = -\frac{262144\,\delta^{16}\mathrm{sech}(\delta\xi)^2\Big(\mathrm{sech}(\delta\xi)^2 - \frac{2}{3}\Big)\,\tau^{2\varrho}}{3\varrho^2}, \tag{42}$$

$$\Omega_3(\xi,\tau) = \Phi_3(\xi)\tau^{3\varrho} = -\frac{268435456\,\delta^{23}\Big(\cosh^2(\delta\xi) - 3\Big)\,\tanh(\delta\xi)\mathrm{sech}(\delta\xi)^4\,\tau^{3\varrho}}{81\varrho^3}, \tag{43}$$

The solution of Equation (36) is obtained in the form of Equation (10).

The exact solution of Equation (36) is given by:

$$\Omega(\xi,\tau) = \frac{4\delta^2}{3}\left(2 - 3\,\tanh^2\left(\delta\xi - \frac{256}{3}\delta^7\tau\right)\right).$$

Example 4. *Consider the time fractional seventh-order KdV Lax model (by setting* $\eta_1 = 140$, $\eta_2 = 70$, $\eta_3 = 280$, $\eta_4 = 70$, $\eta_5 = 70$, $\eta_6 = 42$, $\eta_7 = 14$ *in Equation (19)):*

$$\mathfrak{D}_\tau^\varrho \Omega + 140\,\Omega^3\,\Omega_\xi + 70\,{\Omega_\xi}^3 + 280\,\Omega\,\Omega_\xi\,\Omega_{\xi\xi} + 70\,\Omega^2\,\Omega_{\xi\xi\xi} + 70\,\Omega_{\xi\xi}\,\Omega_{\xi\xi\xi} + 42\,\Omega_\xi\,\Omega_{\xi\xi\xi\xi} + 14\,\Omega\,\Omega_{\xi\xi\xi\xi\xi} + \Omega_{\xi\xi\xi\xi\xi\xi\xi} = 0, \tag{44}$$

where $\varrho \in (0, 1]$ *and with the initial condition*

$$\Omega(\xi, 0) = 2\delta^2\,\mathrm{sec}\,h^2(\delta\xi). \tag{45}$$

Solution: By applying CLADM on Equation (44) discussed in Section 2, we will have

$$\begin{aligned}\Omega(\xi,\tau) &= -\mathfrak{L}_{\varrho}^{-1}\Big[\tfrac{1}{s}\mathfrak{L}_{\varrho}\big(\Omega(\xi,0)+\Omega_{\xi\xi\xi\xi\xi\xi\xi}\big)\Big]-\mathfrak{L}_{\varrho}^{-1}\Big[\tfrac{1}{s}\mathfrak{L}_{\varrho}\big(140\,\Omega^3\,\Omega_{\xi}\\ &\quad +70\,{\Omega_{\xi}}^3+280\,\Omega\,\Omega_{\xi}\,\Omega_{\xi\xi}+70\,\Omega^2\,\Omega_{\xi\xi\xi}+70\,\Omega_{\xi\xi}\,\Omega_{\xi\xi\xi}\\ &\quad +42\,\Omega_{\xi}\,\Omega_{\xi\xi\xi\xi}+14\,\Omega\,\Omega_{\xi\xi\xi\xi\xi}\big)\Big],\end{aligned} \tag{46}$$

$$\begin{aligned}\Omega_{k+1} &= -\mathfrak{L}_{\varrho}^{-1}\Big[\tfrac{1}{s}\mathfrak{L}_{\varrho}\big(\Omega(\xi,0)+\Omega_{\xi\xi\xi\xi\xi\xi\xi_k}\big)\Big]-\mathfrak{L}_{\varrho}^{-1}\Big[\tfrac{1}{s}\mathfrak{L}_{\varrho}\big(140\,\textstyle\sum_{k=0}^{\infty}A_k\\ &\quad +70\,\textstyle\sum_{k=0}^{\infty}B_k+280\,\sum_{k=0}^{\infty}C_k+70\,\sum_{k=0}^{\infty}D_k\\ &\quad +70\,\textstyle\sum_{k=0}^{\infty}E_k+42\,\sum_{k=0}^{\infty}F_k+14\,\sum_{k=0}^{\infty}G_k\big)\Big],\end{aligned} \tag{47}$$

From the initial condition Equation (45), we get

$$\Omega_0(\xi,\tau)=\Phi_0(\xi)=2\,\delta^2\mathrm{sech}(\delta\xi)^2, \tag{48}$$

$$\Omega_1(\xi,\tau)=\Phi_1(\xi)\tau^{\varrho}=\frac{256\,\delta^9\mathrm{sech}(\delta\xi)^2\tanh(\delta\xi)\,\tau^{\varrho}}{\varrho}, \tag{49}$$

$$\Omega_2(\xi,\tau)=\Phi_2(\xi)\tau^{2\varrho}=-\frac{8192\,\delta^{16}\mathrm{sech}(\delta\xi)^2\Big(3\mathrm{sech}(\delta\xi)^2-2\Big)\,\tau^{2\varrho}}{\varrho^2}, \tag{50}$$

$$\Omega_3(\xi,\tau)=\Phi_3(\xi)\tau^{3\varrho}=\frac{2097152\,\delta^{23}\Big(\cosh^2(\delta\xi)-3\Big)\mathrm{sech}(\delta\xi)^4\tanh(\delta\xi)\,\tau^{3\varrho}}{3\varrho^3}, \tag{51}$$

The solution of Equation (44) is obtained in the form of Equation (10).

The exact solution of Equation (44) is given by:

$$\Omega(\xi,\tau)=2\delta^2\,\mathrm{sec}\,h^2\Big(\delta\xi-64\delta^7\tau\Big).$$

4. Result and Discussion

This research investigates a fifth-order and a general seventh-order time-fractional KdV model solved through the Laplace Adobian Decomposition Method (LADM) in a conformable sense. By adjusting the parameters η_i's in the seventh-order KdV model, the study examines specific cases of the time-fractional SKI, KK, and Lax KdV models. The primary objective is to explore their fractional nature, emphasizing dynamic properties and the computational efficiency of the CLADM.

In addition to the analysis of convergence of the series solution, we calculated the terms ψ_k using Theorem 2.

For the fifth-order KdV model solution, we obtained, $\psi_0=\frac{\|\Phi_1\|}{\|\Phi_0\|}=3.2\times10^{-8}<1$, $\psi_1=\frac{\|\Phi_2\|}{\|\Phi_1\|}=0.8<1$, $\psi_2=\frac{\|\Phi_3\|}{\|\Phi_2\|}=4.2667\times10^{-8}<1$.

Similarly, for the seventh-order KdV KK model solution, we have, $\psi_0=\frac{\|\Phi_1\|}{\|\Phi_0\|}=3.99\times10^{-11}<1$, $\psi_1=\frac{\|\Phi_2\|}{\|\Phi_1\|}=6.6917\times10^{-4}<1$, $\psi_2=\frac{\|\Phi_3\|}{\|\Phi_2\|}=3.5506\times10^{-11}<1$.

Also, for seventh-order KdV SKI model solution, we have, $\psi_0=\frac{\|\Phi_1\|}{\|\Phi_0\|}=2.5664\times10^{-9}<1$, $\psi_1=\frac{\|\Phi_2\|}{\|\Phi_1\|}=0.0422<1$, $\psi_2=\frac{\|\Phi_3\|}{\|\Phi_2\|}=2.2985\times10^{-9}<1$.

For the seventh-order KdV Lax model solution, we have, $\psi_0=\frac{\|\Phi_1\|}{\|\Phi_0\|}=1.28\times10^{-9}<1$, $\psi_1=\frac{\|\Phi_2\|}{\|\Phi_1\|}=0.0320<1$, $\psi_2=\frac{\|\Phi_3\|}{\|\Phi_2\|}=1.7067\times10^{-9}<1$.

Hence, all the obtained series solutions are convergent.

The results for the time-fractional fifth-order KdV model (Example 1) underscore the adaptability of the CLADM Method. Table 1 illustrates the comparative analysis of solutions by the CLADM and exact. Numerical comparison of absolute errors Table 2 demonstrate

that the CLADM achieves superior accuracy compared to conventional methods such as the HAM, particularly for higher fractional orders. Figure 1 superposes the surface produced by the proposed CLADM scheme on the exact fractional KdV solution. The two surfaces coincide so closely that they are visually indistinguishable at the plot's resolution, with the highest wave amplitude at the origin gradually tapering off with increasing spatial distance. The fractional parameter ϱ significantly influences wave steepness and amplitude; as ϱ approaches unity, the wave profiles become smoother, aligning with classical dynamics.

A 2D diagram, as shown in Figure 2a,b, showcasing the wave surface levels at various ϱ values highlights the gradual flattening of waves as fractional effects diminish. Figure 3 illustrates the absolute error distribution of the numerical solution for the fifth-order KdV equation over the spatial domain $\xi \in [0, 20]$ and temporal interval $\tau \in [0, 30]$ with parameter $\delta = 0.25$. The graph demonstrates how the numerical approximation deviates from the exact solution. It can be seen that the error remains consistently low throughout the domain, with minor fluctuations over time and space.

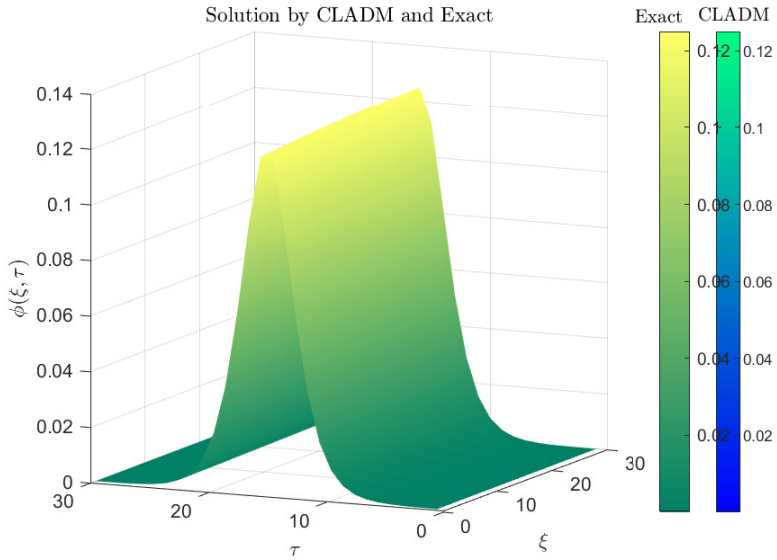
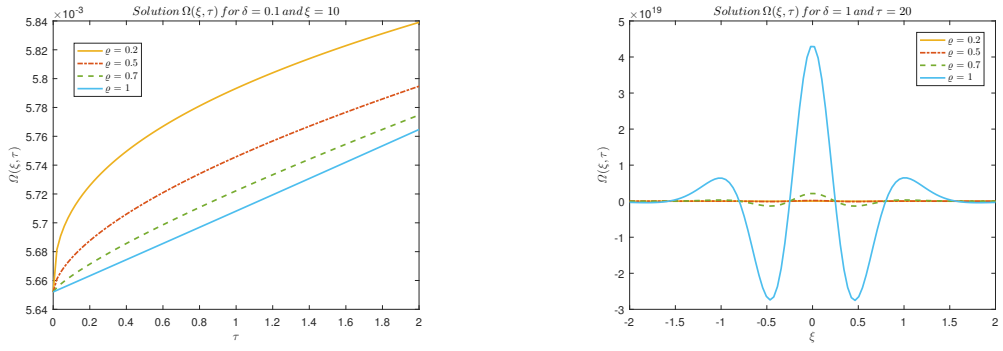


Figure 1. Solution graph of time-fractional fifth-order KdV model by CLADM and Exact.



(**a**) (**b**)

Figure 2. Fifth-order KdV model when (**a**) $\delta = 0.1$ and $\xi = 10$ and (**b**) $\delta = 1$ and $\tau = 20$.

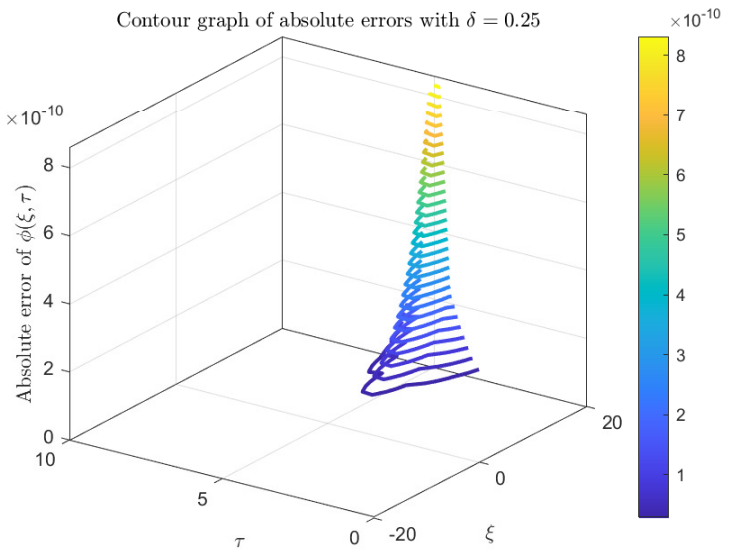


Figure 3. Absolute error graph of time-fractional fifth-order KdV model with $\delta = 0.25$.

Table 1. CLADM numerical comparison of $\Omega(\xi, \tau)$, with a KdV fifth-order fractional model, with $\delta = 0.1$.

ξ	τ	CLADM				Exact	Abs Error
		ϱ = 0.2	ϱ = 0.5	ϱ = 0.7	ϱ = 1		
−2	2	0.019214	0.019217	0.019218	0.019218	0.019218	3.47×10^{-22}
	4	0.019213	0.019216	0.019216	0.019216	0.019216	6.94×10^{-22}
−1.5	2	0.019551	0.019554	0.019555	0.019555	0.019555	0.00
	4	0.019550	0.019553	0.019553	0.019553	0.019553	3.47×10^{-22}
−1	2	0.019798	0.019800	0.019800	0.019800	0.019800	0.00
	4	0.019797	0.019799	0.019799	0.019799	0.019799	6.94×10^{-22}
−0.5	2	0.019948	0.019949	0.019949	0.019949	0.019949	6.94×10^{-22}
	4	0.019948	0.019949	0.019949	0.019949	0.019949	6.94×10^{-22}
0	2	0.020000	0.020000	0.020000	0.020000	0.020000	3.47×10^{-22}
	4	0.020000	0.020000	0.020000	0.020000	0.020000	3.47×10^{-22}
0.5	2	0.019952	0.019951	0.019951	0.019951	0.019951	6.94×10^{-22}
	4	0.019952	0.019951	0.019951	0.019951	0.019951	3.47×10^{-22}
1	2	0.019805	0.019803	0.019803	0.019803	0.019803	6.94×10^{-22}
	4	0.019805	0.019804	0.019804	0.019804	0.019804	6.94×10^{-22}
1.5	2	0.019562	0.019559	0.019559	0.019559	0.019559	0.00
	4	0.019563	0.019560	0.019560	0.019560	0.019560	3.47×10^{-22}
2	2	0.019228	0.019224	0.019224	0.019223	0.019223	0.00
	4	0.019229	0.019226	0.019225	0.019226	0.019226	3.47×10^{-22}

Table 2. CLADM numerical comparison of $\Omega(\xi, \tau)$, with a KdV fifth-order fractional model, at $\xi = 10$ and $\delta = 0.15$.

τ	CLADM				Exact	Abs Error
	$\varrho = 0.2$	$\varrho = 0.5$	$\varrho = 0.7$	$\varrho = 1$		
0.1	0.026977	0.026873	0.026858	0.026851	0.026851	1.73×10^{-22}
0.6	0.027034	0.026911	0.026888	0.026871	0.026871	1.73×10^{-22}
1.1	0.027058	0.026933	0.026910	0.026892	0.026892	0.00
1.6	0.027074	0.026951	0.026929	0.026913	0.026913	5.20×10^{-22}
2.1	0.027087	0.026967	0.026946	0.026933	0.026933	1.73×10^{-22}

In the analysis of the KdV KK model (Example 2), absolute errors are calculated for various time and space parameters and are compared against results obtained using the exact solution. The comparative results Table 3 consistently highlight the precision of the CLADM, demonstrating significantly lower errors. Furthermore, as shown in Table 4, errors decrease with increasing fractional order, suggesting enhanced accuracy of wave propagation models in near-classical regimes. The graphical analysis offers additional insights into the wave behavior. For the Lax KdV model, a 3D visualization of approximate solutions and exact solution Figure 4 reveals that wave amplitude peaks at $\xi = 0$ and diminishes with increasing distance. Fractional order ϱ plays a critical role in wave dynamics, as illustrated in Figure 5a, where higher ϱ values result in flatter wave profiles, indicating reduced steepness. Additionally, the 2D diagram in Figure 5b demonstrates that increasing ϱ leads to an enlargement in wave surface levels while dampening oscillations with distance from the origin. Figure 6 presents the absolute error profile for the numerical solution of the seventh-order KdV-KK equation over the spatial domain $\xi \in [0, 20]$ and time interval $\tau \in [0, 30]$ with parameter $\delta = 0.3$. From the figure, it is evident that the error remains extremely low throughout the entire domain. This demonstrates the high accuracy and numerical stability of the computational scheme.

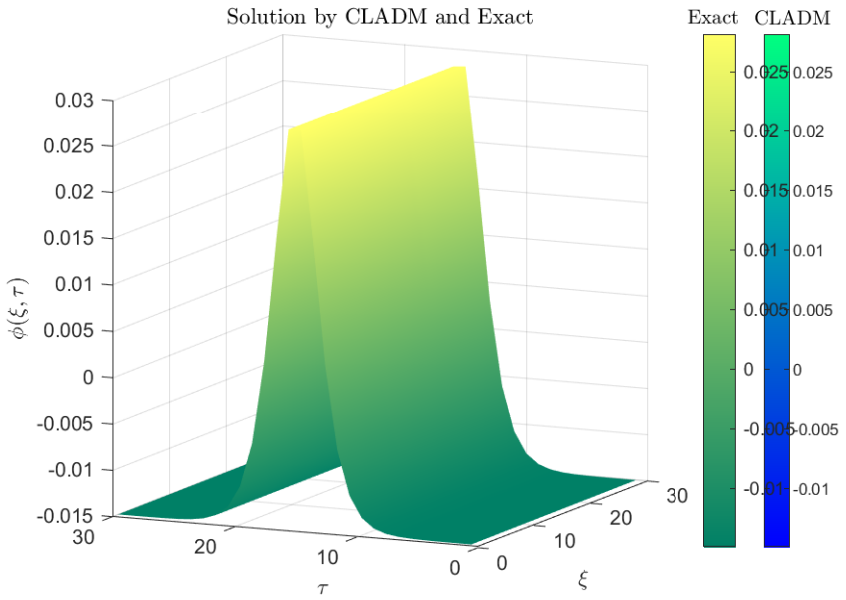


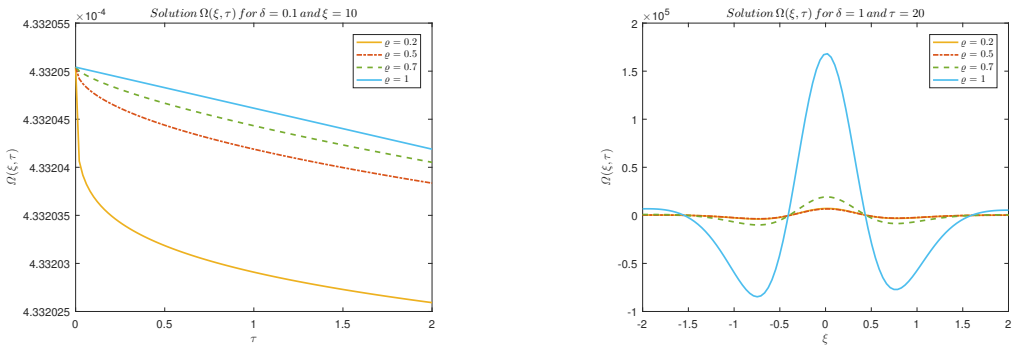
Figure 4. Solution graph of time-fractional KdV seventh-order KK model by CLADM and Exact.

Table 3. CLADM numerical comparison of $\Omega(\xi, \tau)$, with a KdV seventh-order KK fractional model, with $\delta = 0.1$.

ξ	τ	CLADM				Exact	Abs Error
		ϱ = 0.2	ϱ = 0.5	ϱ = 0.7	ϱ = 1		
−2	2	0.003139	0.003139	0.003139	0.003139	0.003139	0.00
	4	0.003139	0.003139	0.003139	0.003139	0.003139	0.00
−1.5	2	0.003223	0.003223	0.003223	0.003222	0.003222	0.00
	4	0.003223	0.003223	0.003223	0.003223	0.003223	0.00
−1	2	0.003284	0.003284	0.003284	0.003284	0.003284	0.00
	4	0.003284	0.003284	0.003284	0.003284	0.003284	0.00
−0.5	2	0.003321	0.003321	0.003321	0.003321	0.003321	0.00
	4	0.003321	0.003321	0.003321	0.003321	0.003321	0.00
0	2	0.003333	0.003333	0.003333	0.003333	0.003333	0.00
	4	0.003333	0.003333	0.003333	0.003333	0.003333	4.34×10^{-20}
0.5	2	0.003321	0.003321	0.003321	0.003321	0.003321	0.00
	4	0.003321	0.003321	0.003321	0.003321	0.003321	0.00
1	2	0.003284	0.003284	0.003284	0.003284	0.003284	0.00
	4	0.003284	0.003284	0.003284	0.003284	0.003284	0.00
1.5	2	0.003222	0.003222	0.003222	0.003222	0.003222	0.00
	4	0.003222	0.003222	0.003222	0.003222	0.003222	0.00
2	2	0.003139	0.003139	0.003139	0.003139	0.003139	0.00
	4	0.003139	0.003139	0.003139	0.003139	0.003139	0.00

Table 4. CLADM numerical comparison of $\Omega(\xi, \tau)$, with a KdV seventh-order KK fractional model, at $\xi = 5$ and $\delta = 0.15$.

τ	CLADM				Exact	Abs Error
	ϱ = 0.2	ϱ = 0.5	ϱ = 0.7	ϱ = 1		
0.1	0.002962	0.002962	0.002962	0.002962	0.002962	0.00
0.6	0.002962	0.002962	0.002962	0.002962	0.002962	1.73×10^{-22}
1.1	0.002961	0.002962	0.002962	0.002962	0.002962	3.47×10^{-22}
1.6	0.002961	0.002962	0.002962	0.002962	0.002962	1.73×10^{-22}
2.1	0.002961	0.002962	0.002962	0.002962	0.002962	1.73×10^{-22}



(**a**) (**b**)

Figure 5. KdV seventh-order KK model when (**a**) $\delta = 0.1$ and $\xi = 10$ and (**b**) $\delta = 1$ and $\tau = 20$.

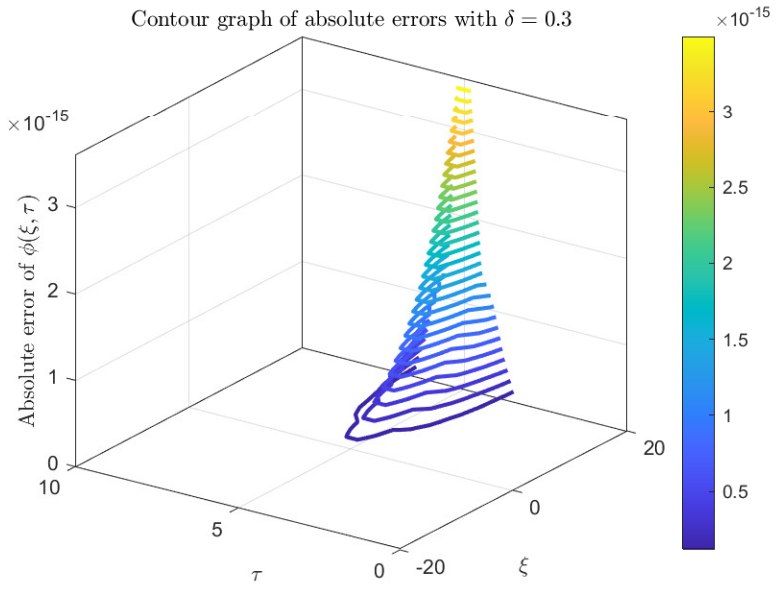


Figure 6. Absolute error graph of time-fractional seventh-order KdV KK model with $\delta = 0.3$.

For the KdV SKI model (Example 3), a similar trend is observed. Numerical comparison of distinct fractional order ϱ and absolute error Tables 5 and 6 validate the efficiency of the CLADM over HAM [3], with reduced error magnitudes as fractional order increases. The 3D solution Figure 7 further confirm the robustness of the CLADM. In Figure 8a, higher ϱ values correlate with increased wave amplitudes. Additionally, the 2D graphs in Figure 8b for fixed time periods highlight the same trends, underscoring the model's fidelity in capturing intricate wave dynamics. Figure 9 presents the absolute error profile for the numerical solution of the seventh-order KdV-SKI equation over the spatial domain $\xi \in [0, 20]$ and time interval $\tau \in [0, 30]$ with parameter $\delta = 0.1$. Compared to other fifth- and seventh-order models, this result shows a relatively higher error, which can be attributed to the lower dispersion strength.

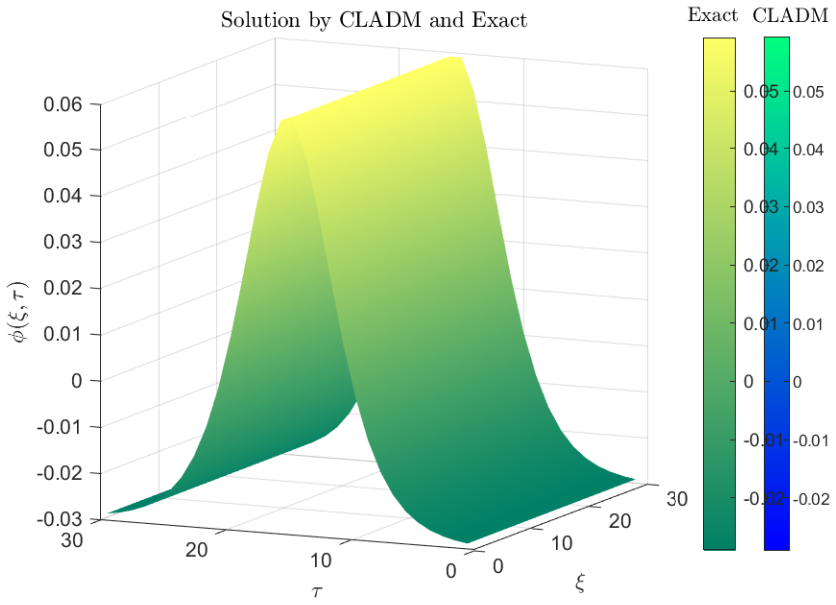


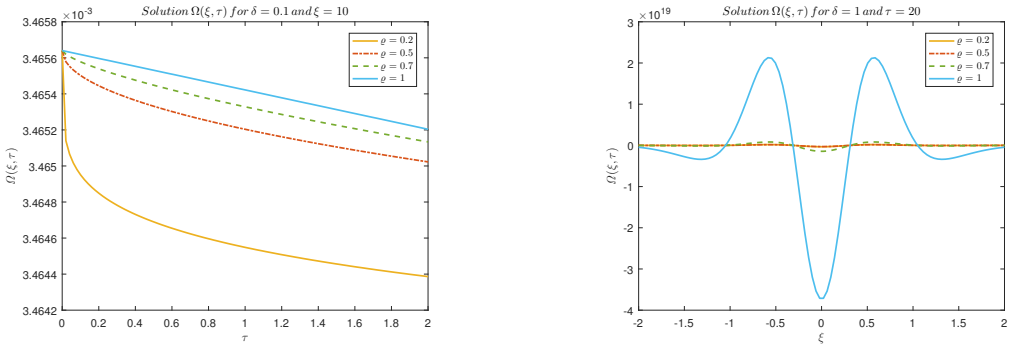
Figure 7. Solution graph of time-fractional KdV seventh-order SKI model by CLADM and Exact.

Table 5. CLADM numerical comparison of $\Omega(\xi, \tau)$, with a KdV seventh-order SKI fractional model, with $\delta = 0.1$.

ξ	τ	CLADM				Exact	Abs Error
		ϱ = 0.2	ϱ = 0.5	ϱ = 0.7	ϱ = 1		
0.1	1	0.026663	0.026663	0.026663	0.026663	0.026663	1.37×10^{-10}
	2	0.026663	0.026663	0.026663	0.026663	0.026663	2.73×10^{-10}
	3	0.026663	0.026663	0.026663	0.026663	0.026663	4.10×10^{-10}
0.5	1	0.026567	0.026567	0.026567	0.026567	0.026567	6.80×10^{-10}
	2	0.026567	0.026567	0.026567	0.026567	0.026567	1.36×10^{-9}
	3	0.026567	0.026567	0.026567	0.026567	0.026567	2.04×10^{-9}
0.9	1	0.026344	0.026344	0.026344	0.026344	0.026344	1.22×10^{-9}
	2	0.026344	0.026344	0.026344	0.026344	0.026345	2.43×10^{-9}
	3	0.026344	0.026344	0.026344	0.026344	0.026345	3.65×10^{-9}
1.3	1	0.025998	0.025998	0.025998	0.025998	0.025998	1.74×10^{-9}
	2	0.025998	0.025998	0.025998	0.025998	0.025998	3.47×10^{-9}
	3	0.025998	0.025998	0.025998	0.025998	0.025998	5.21×10^{-9}
1.9	1	0.025256	0.025256	0.025257	0.025257	0.025257	2.47×10^{-9}
	2	0.025256	0.025256	0.025256	0.025256	0.025257	4.95×10^{-9}
	3	0.025256	0.025256	0.025256	0.025256	0.025257	7.42×10^{-9}

Table 6. CLADM numerical comparison of $\Omega(\xi, \tau)$, with a KdV seventh-order SKI fractional model, at $\xi = 10$ and $\delta = 0.15$.

τ	CLADM				Exact	Abs Error
	ϱ = 0.2	ϱ = 0.5	ϱ = 0.7	ϱ = 1		
0.1	−0.013750	−0.013739	−0.013738	−0.013736	−0.013736	8.59×10^{-9}
0.6	−0.013756	−0.013743	−0.013741	−0.013734	−0.013734	5.15×10^{-8}
1.1	−0.013758	−0.013745	−0.013743	−0.013732	−0.013732	9.44×10^{-8}
1.6	−0.013760	−0.013747	−0.013745	−0.013730	−0.013730	1.37×10^{-7}
2.1	−0.013761	−0.013749	−0.013747	−0.013727	−0.013727	1.80×10^{-7}



(**a**) (**b**)

Figure 8. KdV seventh-order SKI model when (**a**) $\delta = 0.1$ and $\xi = 10$ and (**b**) $\delta = 1$ and $\tau = 20$.

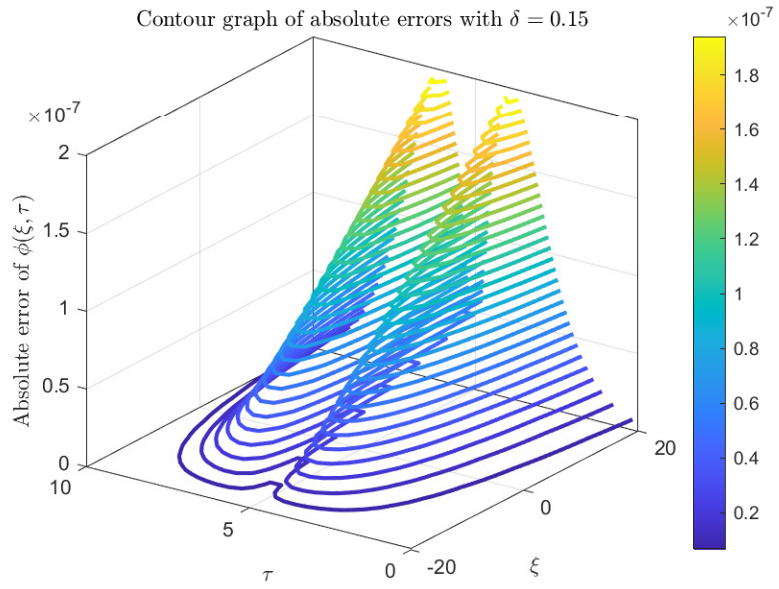


Figure 9. Absolute error graph of time-fractional seventh-order KdV SKI model with $\delta = 0.1$.

In the KdV Lax model (Example 4), numerical comparison of absolute error Tables 7 and 8 reinforce the reliability of the CLADM for complex fractional models. The 3D solution and error visualizations Figure 10 reflect the accuracy of the method, while Figure 11a,b illustrates how the water surface level increases with higher fractional parameters. Figure 12 presents the absolute error profile for the numerical solution of the seventh-order KdV-Lax equation over the spatial domain $\xi \in [0, 20]$ and time interval $\tau \in [0, 30]$ with parameter $\delta = 0.2$. From the figure, it is evident that the error remains extremely low throughout the entire domain.

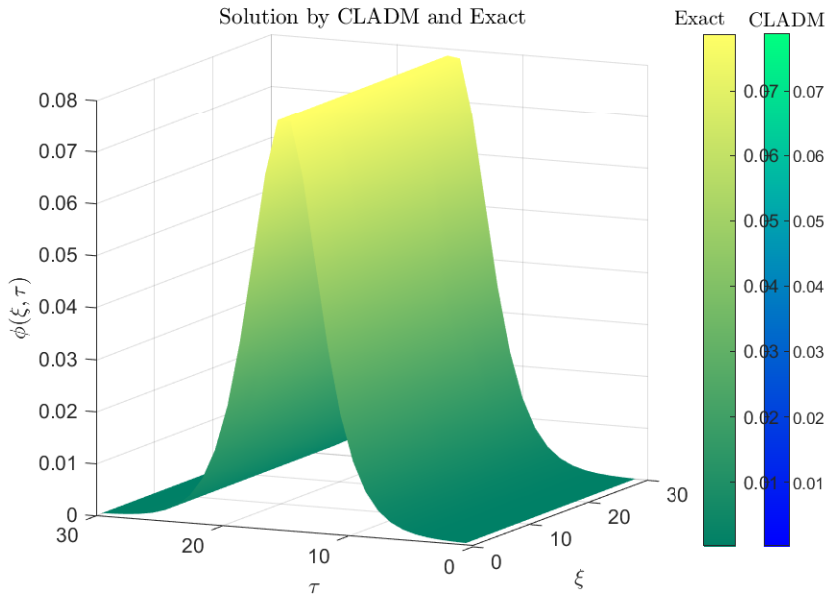


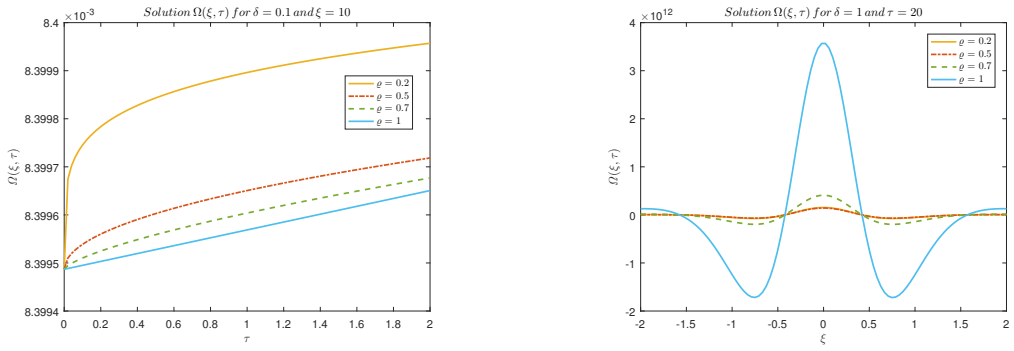
Figure 10. Solution graph of time-fractional KdV seventh-order Lax model by CLADM and Exact.

Table 7. CLADM numerical comparison of $\Omega(\xi, \tau)$, with a KdV seventh-order Lax fractional model, with $\delta = 0.1$.

ξ	τ	CLADM				Exact	Abs Error
		ϱ = 0.2	ϱ = 0.5	ϱ = 0.7	ϱ = 1		
−2	2	0.019221	0.019221	0.019221	0.019221	0.019221	3.47×10^{-22}
	4	0.019221	0.019221	0.019221	0.019221	0.019221	3.47×10^{-22}
−1.5	2	0.019556	0.019557	0.019557	0.019557	0.019557	3.47×10^{-22}
	4	0.019556	0.019557	0.019557	0.019557	0.019557	0.00
−1	2	0.019801	0.019801	0.019801	0.019801	0.019801	3.47×10^{-22}
	4	0.019801	0.019801	0.019801	0.019801	0.019801	6.94×10^{-22}
−0.5	2	0.019950	0.019950	0.019950	0.019950	0.019950	0.00
	4	0.019950	0.019950	0.019950	0.019950	0.019950	3.47×10^{-22}
0	2	0.020000	0.020000	0.020000	0.020000	0.020000	3.47×10^{-22}
	4	0.020000	0.020000	0.020000	0.020000	0.020000	6.94×10^{-22}
0.5	2	0.019950	0.019950	0.019950	0.019950	0.019950	6.94×10^{-22}
	4	0.019950	0.019950	0.019950	0.019950	0.019950	3.47×10^{-22}
1	2	0.019801	0.019801	0.019801	0.019801	0.019801	0.00
	4	0.019801	0.019801	0.019801	0.019801	0.019801	6.94×10^{-22}
1.5	2	0.019557	0.019557	0.019557	0.019557	0.019557	3.47×10^{-22}
	4	0.019557	0.019557	0.019557	0.019557	0.019557	0.00
2	2	0.019221	0.019221	0.019221	0.019221	0.019221	3.47×10^{-22}
	4	0.019221	0.019221	0.019221	0.019221	0.019221	3.47×10^{-22}

Table 8. CLADM numerical comparison of $\Omega(\xi, \tau)$, with a KdV seventh-order Lax fractional model, at $\xi = 5$ and $\delta = 0.15$.

τ	CLADM				Exact	Abs Error
	ϱ = 0.2	ϱ = 0.5	ϱ = 0.7	ϱ = 1		
0.1	0.002962	0.002962	0.002962	0.002962	0.002962	5.20×10^{-22}
0.6	0.002962	0.002962	0.002962	0.002962	0.002962	0.00
1.1	0.002961	0.002962	0.002962	0.002962	0.002962	0.00
1.6	0.002961	0.002962	0.002962	0.002962	0.002962	0.00
2.1	0.002961	0.002962	0.002962	0.002962	0.002962	3.47×10^{-22}



(**a**) (**b**)

Figure 11. KdV seventh-order Lax model when (**a**) $\delta = 0.1$ and $\xi = 10$ and (**b**) $\delta = 1$ and $\tau = 20$.

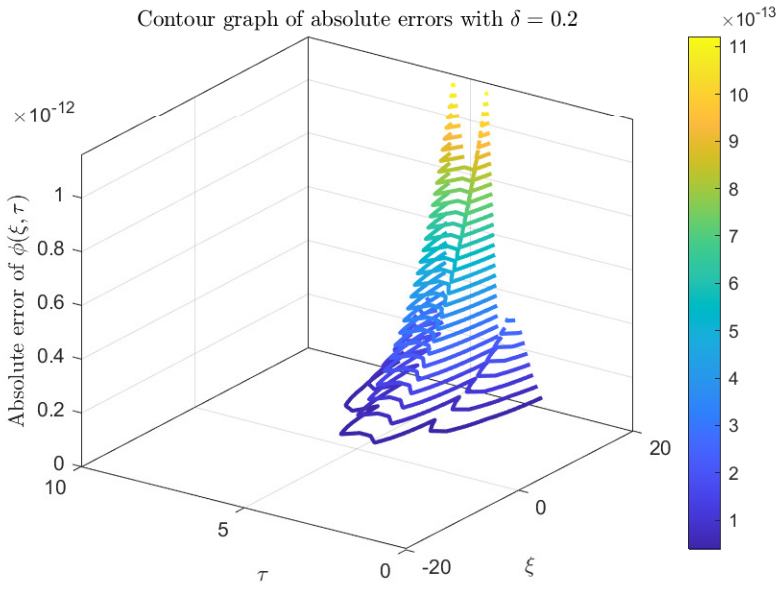


Figure 12. Absolute error graph of time-fractional seventh-order KdV Lax model with $\delta = 0.2$.

5. Conclusions

This study demonstrates the effectiveness of the Conformable Laplace Adobian Decomposition Method (CLADM) in solving generalized time fractional seventh-order Sawada–Kotera–Ito, Kaup–Kuperschmidt, Lax, and the fifth-order KdV models. The results highlight the significant impact of fractional parameters on wave dynamics, with increasing ϱ yielding smoother wave profiles and reduced oscillations, aligning closely with classical integer-order behavior. Comparisons with existing methods, such as HAM and HLM, confirm CLADM's superior accuracy in minimizing absolute errors. Graphical and numerical analyses validate its versatility in addressing complex fractional dynamics and initial conditions across different models. In conclusion, CLADM is a reliable and efficient approach for solving fractional-order nonlinear equations. It handles any problem whose fractional operator admits a Laplace image and whose nonlinearity is analytic. That spans single- and multi-term FODEs, time-fractional PDEs, coupled or delay systems, integro-differential forms, and even variable-order kernels. Its adaptability suggests strong potential for future research into multi-dimensional solitonic systems and other nonlinear wave phenomena.

Author Contributions: Methodology, P.V.T. and A.P.; Software, A.P.; Validation, P.V.T. and A.P.; Formal analysis, P.V.T. and T.P.; Investigation, A.P. and T.P.; Writing—original draft, A.P.; Writing—review & editing, T.P.; Supervision, P.V.T. All authors have read and agreed to the published version of the manuscript.

Funding: This research received no external funding.

Data Availability Statement: The original contributions presented in this study are included in the article. Further inquiries can be directed to the corresponding author.

Conflicts of Interest: There are no conflicts of interests regarding the publication of this manuscript.

References

1. Qayyum, M.; Ahmad, E.; Saeed, S.T.; Akgul, A.; Riaz, M.B. Traveling wave solutions of generalized seventh-order time-fractional kdv models through he-laplace algorithm. *Alex. Eng. J.* **2023**, *70*, 1–11. [CrossRef]
2. Alzaid, N.A.; Alrayiqi, B.A. Approximate solution method of the seventh order kdv equations by decomposition method. *J. Appl. Math. Phys.* **2019**, *7*, 2148–2155. [CrossRef]

3. Arora, R.; Sharma, H. Application of ham to seventh order kdv equations. *Int. J. Syst. Assur. Eng. Manag.* **2016**, *9*, 131–138. [CrossRef]
4. Bruzon, M.; Marquez, A.; Garrido, T.; Recio, E.; de la Rosa, R. Conservation laws for a generalized seventh order kdv equation. *J. Comput. Appl. Math.* **2019**, *354*, 682–688. [CrossRef]
5. Joshi, N.; Lustri, C.J. Generalized solitary waves in a finite-difference korteweg-de vries equation. *Stud. Appl. Math.* **2019**, *142*, 359–384. [CrossRef]
6. Guner, O. New exact solutions for the seventh-order time fractional sawada–kotera–ito equation via various methods. *Waves Random Complex Media* **2018**, *30*, 441–457. [CrossRef]
7. Mancas, S.C.; Hereman, W.A. Traveling wave solutions to fifth- and seventh-order korteweg–de vries equations: Sech and cn solutions. *J. Phys. Soc. Jpn.* **2018**, *87*, 114002. [CrossRef]
8. Wang, G.; Liu, Y.; Wu, Y.; Su, X. Symmetry analysis for a seventh-order generalized kdv equation and its fractional version in fluid mechanics. *Fractals* **2020**, *28*, 2050044. [CrossRef]
9. Handibag, S.; Karande, B.D. Existence the solutions of some fifth-order kdv equation by laplace decomposition method. *Am. J. Comput. Math.* **2013**, *3*, 80–85. [CrossRef]
10. Wang, Z.; Sun, L.; Hua, R.; Su, L.; Zhang, L. Time-fractional generalized fifth-order kdv equation: Lie symmetry analysis and conservation laws. *Front. Phys.* **2023**, *11*, 1133754. [CrossRef]
11. Liu, T. Exact solutions to time-fractional fifth order kdv equation by trial equation method based on symmetry. *Symmetry* **2019**, *11*, 742. [CrossRef]
12. Rehman, M.F.U.; Gu, Y.; Yuan, W. Exact analytical solutions of generalized fifth-order kdv equation by the extended com-plex method. *J. Funct. Spaces* **2021**, *2021*, 1–9. [CrossRef]
13. Ali, U.; Ahmad, H.; Abu-Zinadah, H. Soliton solutions for nonlinear variable-order fractional korteweg–de vries (kdv) equation arising in shallow water waves. *J. Ocean Eng. Sci.* **2022**, *9*, 50–58. [CrossRef]
14. Shakeel, A.M.; Alaoui, M.K.; Zidan, A.M.; Shah, N.A. Closed form solutions for the generalized fifth-order kdv equation by using the modified exp-function method. *J. Ocean Eng. Sci.* **2022**. [CrossRef]
15. Akbulut, A.; Kaplan, M.; Kaabar, M.K. New conservation laws and exact solutions of the special case of the fifth-order kdv equation. *J. Ocean Eng. Sci.* **2022**, *7*, 377–382. [CrossRef]
16. Verma, L.; Meher, R.; Avazzadeh, Z.; Nikan, O. Solution for generalized fuzzy fractional kortewege-de varies equation us-ing a robust fuzzy double parametric approach. *J. Ocean Eng. Sci.* **2023**, *8*, 602–622. [CrossRef]
17. Kurulay, M.; Bayram, M. Approximate analytical solution for the fractional modified kdv by differential transform method. *Commun. Nonlinear Sci. Numer. Simul.* **2010**, *15*, 1777–1782. [CrossRef]
18. Wang, G.-W.; Liu, X.-Q.; Zhang, Y.-Y. Lie symmetry analysis to the time fractional generalized fifth-order kdv equation. *Commun.—Tions Nonlinear Sci. Numer. Simul.* **2013**, *18*, 2321–2326. [CrossRef]
19. Nazari-Golshan, A. Derivation and solution of space fractional modified korteweg de vries equation. *Commun. Nonlinear Sci. Numer. Simul.* **2019**, *79*, 104904. [CrossRef]
20. Alshammari, M.; Iqbal, N.; Mohammed, W.W.; Botmart, T. The solution of fractional-order system of kdv equations with exponential-decay kernel. *Results Phys.* **2022**, *38*, 105615. [CrossRef]
21. Cao, H.; Cheng, X.; Zhang, Q. Numerical simulation methods and analysis for the dynamics of the time-fractional kdv equation. *Phys. D Nonlinear Phenom.* **2024**, *460*, 134050. [CrossRef]
22. Yousif, M.A.; Hamasalh, F.K.; Zeeshan, A.; Abdelwahed, M. Efficient simulation of time-fractional korteweg-de vries equation via conformable-caputo non-polynomial spline method. *PLoS ONE* **2024**, *19*, e0303760. [CrossRef] [PubMed]
23. Dwivedi, M.; Sarkar, T. Numerical method for the zero dispersion limit of the fractional korteweg-de vries equation. *arXiv* **2024**. [CrossRef]
24. Gu, Y. High-order numerical method for the fractional korteweg-de vries equation using the discontinuous galerkin method. *AIMS Math.* **2025**, *10*, 1367–1383. [CrossRef]
25. Khalil, R.; Al Horani, M.; Yousef, A.; Sababheh, M. A new definition of fractional derivative. *J. Comput. Appl. Math.* **2014**, *264*, 65–70. [CrossRef]
26. Ahmed, S.A. An efficient new technique for solving nonlinear problems involving the conformable fractional derivatives. *J. Appl. Math.* **2024**, *2024*, 5958560. [CrossRef]
27. Hashemi, M. Invariant subspaces admitted by fractional differential equations with conformable derivatives. *Chaos Solitons Fractals* **2018**, *107*, 161–169. [CrossRef]
28. Osman, W.M.; Elzaki, T.M.; Siddig, N.A. Modified double conformable laplace transform and singular fractional pseudo-hyperbolic and pseudo-parabolic equations. *J. King Saud Univ.—Sci.* **2021**, *33*, 101378. [CrossRef]
29. Ayata, M.; Ozkan, O. A new application of conformable laplace decomposition method for fractional newell-whitehead-segel equation. *AIMS Math.* **2020**, *5*, 4702–4712. [CrossRef]
30. Abdeljawad, T. On conformable fractional calculus. *J. Comput. Appl. Math.* **2015**, *279*, 57–66. [CrossRef]

31. Silva, F.S.; Moreira, D.M.; Moret, M.A. Conformable laplace transform of fractional differential equations. *Axioms* **2018**, *7*, 55. [CrossRef]
32. Maisuria, M.A.; Tandel, P.V. Mathematical modelling and application of reduced differential transform method for river pollution. *Ratio Math.* **2023**, *47*, 342–366. [CrossRef]
33. More, P.A.; Tandel, P.V. Study of parametric effect on saturation rate in imbibition phenomenon for various porous materials. *J. Ocean Eng. Sci.* **2024**, *9*, 278–292. [CrossRef]
34. Liu, C.; Dai, Z. Exact soliton solutions for the fifth-order sawada–kotera equation. *Appl. Math. Comput.* **2008**, *206*, 272–275. [CrossRef]
35. Guo, Y.; Li, D.; Wang, J. The new exact solutions of the fifth-order sawada–kotera equation using three wave method. *Appl. Math. Lett.* **2019**, *94*, 232–237. [CrossRef]

Disclaimer/Publisher's Note: The statements, opinions and data contained in all publications are solely those of the individual author(s) and contributor(s) and not of MDPI and/or the editor(s). MDPI and/or the editor(s) disclaim responsibility for any injury to people or property resulting from any ideas, methods, instructions or products referred to in the content.